An Accident-Avoidance Full Velocity Difference Model for Animating Realistic Street-Level Traffic in Rural Scenes

Abstract

Most of existing traffic simulation efforts focus on urban regions with a coarse 2-D representation, relatively few works have been conducted to simulate realistic 3-D traffic flows on a large, complex road web in rural scenes. In this paper we propose a novel agent-based approach called Accident-Avoidance Full Velocity Difference Model (abbreviated as AA-FVDM) to simulate realistic street-level rural traffics, on top of the existing FVDM model. The main distinction between FVDM and AA-FVDM is: FVDM cannot handle a critical real-world traffic problem while AA-FVDM settles this problem and retains the essence of FVDM. Our proposed AA-FVDM model can simulate diverse individualistic driving behaviors, which continuum methods cannot simulate. Through numerous simulation experiments, we demonstrate that besides addressing a previously unaddressed real-world traffic problem, our AA-FVDM method efficiently (real-time) simulates large-scale traffic flows (tens of thousands of vehicles) with realistic, smooth effects. Furthermore, we validate our method using real-world traffic data, and the validation results show that our method measurably outperforms state-of-the-art traffic simulation methods.

Keywords: traffic animation, microscopic model, vehicle flow

1 Introduction

Traffic simulation techniques can play a key part in urban development and planning, road network design, road systems and roadside hardware. At the same time, it is also of great importance in improving and completing traffic laws, guidelines and policy to explore the motion of traffic flows. In addition to these, it is of growing need to apply realistic street-level traffic to applications; for example, virtual traffic driving for driving instructions, virtual tourism, special effects for movies, racing games and so on. However, even though there are plenty of traffic simulation models, most existing traffic simulators (e.g., the work of [1]) utilize a two-dimensional abstract representation and center on urban-related traffic, therefore a system for animating realistic traffic in rural places is practically needed for its critical role in society functioning.

Although continuum-based methods [2–7] are fast and efficient, they have the following limitations such as lacking the diversity of individualistic behavior and difficulty to handle scenes with complicated road networks due to their inherent characteristics and inflexibility. Therefore, agent-based methods (or called microscopic methods) [8–15] have been the most popular traffic simulation approaches in recent years. Through a number of delicately designed rules, agent-based methods are capable of simulating: (i) detailed behavior including anisotropic drivers, and (ii) individualistic behavior with complex dynamics.

Among various agent-based approaches, car-following models have achieved noticeable successes in recent years, such as the optimal velocity model (OVM) [11], the generalized force model (GFM) [12], and the full velocity difference model (FVDM) [8]. In particular, FVDM [8] that is built on top of OVM and GFM is

an effective traffic simulation model, and it can simulate realistic traffic at most cases. However, it fails to handle the following situation (called **close-car-braking circumstance**): If the distance between the leading car and the following car is small and their speeds are quite close, and the leading car makes a sharp brake for an accident ahead or the red traffic light at a crossroad, in this case, accidents often can be avoided in real world. However, in the FVDM simulation, the two cars will collide after a few seconds (refer to Figures 8 and 11 in Section 5). It should be noted that close-car-braking circumstance plays a pivotal role in the operating of a realistic traffic system, since this phenomenon often occurs in real world traffic.

Motivated by the above problem, we propose a novel approach called Accident-Avoidance FVDM (AA-FVDM) that retains the essence of FVDM while elegantly handling the above **close-car-braking circumstance**. From a technical perspective, our approach essentially introduces two force terms ("psychological force" and "body force") if the distance between the leading car and the following car is within a pre-specified threshold. Our approach generates suitable deceleration to the following vehicle, which can timely avoid unnecessary accidents in the **close-car-braking circumstance**. On the other hand, lane changing maneuver was mostly either modeled as an instantaneous event [1, 16–19], or an action with uniform duration [20]. Moreover, existing lane changing models typically focus on making decisions and overlook the execution of the maneuvering process [21]. In this work, we introduce a novel scheme to animate the detailed course of lane changing behavior, particularly, the execution course covering dynamics and constraints of a lane changing vehicle.

The **main contributions** of this work are:

1. A novel approach to address an important yet largely underexplored traffic simulation problem the "close-car-braking circumstance" while preserving the advantages of FVDM;

2. A new scheme to animate lane changing maneuvering process in detail, especially the execution course.

To evaluate our approach, we build a traffic simulation system that can simulate large-scale lifelike rural traffic flows at interactive rates in complex road networks containing flyovers, suspension bridges, curving tunnels, and many other road structures. We further compare real-world traffic data with the simulation results of a variety of traffic models (including our approach). The comparison results demonstrate that our method can measurably outperform many state-of-the-art models.

2 Related Work

2.1 Traffic Simulation Models

Visualization and animation of vehicles and traffic flows have attracted increasing interests [7, 22, 23] in graphics community during the past decade. Technically speaking, there are three roughly classified categories for traffic simulation: microscopic, macroscopic, and mesoscopic. Among the three categories, the least common method is mesoscopic, which is based on Boltzmann-type mesoscale equations and has a continuum description. Prigogine et al. [24] came up with the idea as the seminal work. Afterwards, researchers proposed various variations or extensions to further improve the work [25, 26].

To date, agent-based techniques are the most popular methods for traffic simulation, where each vehicle is regarded as an agent and a set of advanced rules are employed to generate natural vehicular behavior. Gerlough [9] is among the first to discuss car-following rules. Subsequently, Newell [10] further merged more characteristics into agent-based models. Recently, Jiang et al. [8] developed a full velocity difference model (FVDM) due to several shortcomings in OVM [11] and GFM [12]. However, their FVDM model will result in unnecessary collisions in the **close-car-braking circumstance** (described in Section 1). In addition, cellular automata was also applied to the field of traffic dynamics [15]. For more detailed descriptions of various agent-based traffic simulation models, please refer to recent surveys [13, 14].

Macroscopic is also called continuum-based. Lighthill et al. [2] and Richards [3] did the earliest work independently in this direction, thus this model is often called the LWR model. LWR model is only based on traffic density, so Payne et al. [4] created a second-order system of equations called the PW model. Later, researchers made various extension [5, 6] to the PW model.

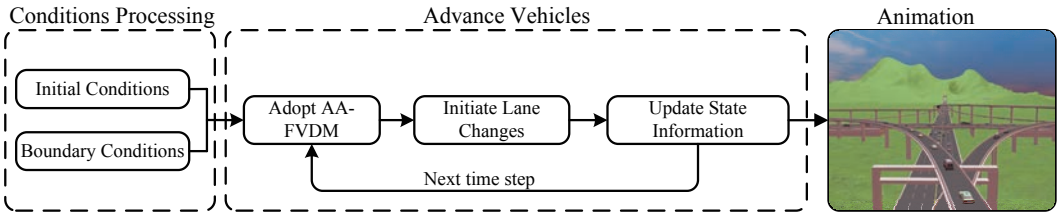

Figure 1: The overview for our system.

2.2 Lane Changing Models

Most of lane changing models typically focus on agent-based traffic models. Nagel et al. [27] summarize different approaches for lane changing and proposed a general scheme, with which realistic lane changing rules could be developed. Huang [28] use cellular automaton to model lane-changing behavior on multilane highways. Hidas [20] developed a novel lane change model to simulate vehicle interactions using intelligent agent concepts. Kesting et al. [19] presented a general lane-changing model for car-following traffic models by minimizing overall braking induced by lane changes. Most of these existing lane changing models center around drivers' decisions and generally overlook the execution of lane changing procedure [21]. In contrast, in this work, we adopt a simple decision-making model and emphatically represent the details of the lane changing course.

3 Preliminaries

3.1 Basic Definitions

Definition 1: The road network consists of a series of roads, $RN = \bigcup \{R_z | z = 1, 2 \ldots\}$.

Definition 2: There are a few lanes on a single road, and we describe lanes with several properties, for instance, the maximum speed $v_{\max}$, the adjacent lanes ls, and R are the roads the lane belongs to. The properties of lane j can be described as $P_j = \{v_{\max}, ls, R\}$.

Definition 3: Every lane j has a number of cars, $Cars_k = \bigcup \{c_i | i = 1, 2, 3 \ldots\}$; because our model is agent-based, we need some further information to depict its state, including position, velocity, length, detecting radii (see Definition 4) and vehicle types. For simplicity, it can be represented as $c_i = \{p_i, v_i, l_i, r_i, t_i\}$.

Definition 4: There is a virtual ellipse encircling each car, and we regard its semimajor axis as the vehicle's detecting radii. We apply the following formula to compute each car's detecting radii r_i.

$$r_i = \gamma l_i \tag{1}$$

Definition 5: Before actually animating vehicles' behaviour, it is necessary to set the initial conditions and boundary conditions, including position, velocity, type, length and so forth. Boundary conditions include the length of lanes, and how to handle cars which come and go across the boundary of the simulation area.

3.2 Full Velocity Difference Model

In 2001, a full velocity difference model (FVDM) was presented by Jiang et al. [8] by considering the negative velocity difference based on GFM. So, the derivation process of the FVDM is like this:

$$\begin{aligned} \frac{dv_i}{dt} &= \kappa[v_i^0 - v_i] + \kappa[V(s_i) - v_i^0] \\ &\quad - \lambda\Theta(\Delta v_i)\Delta v_i - \lambda\Theta(-\Delta v_i)\Delta v_i \\ &= \kappa[V(s_i) - v_i] - \lambda\Delta v_i \end{aligned} \tag{2}$$

where κ, λ are constants, $s_i = x_{i-1} - x_i - l_{i-1}$ is the net spacing between the leader and the follower, $V(s_i) = V_1 + V_2 \tanh(C_1 s_i - C_2)$ is the optimal velocity function, $\Delta v_i = v_i - v_{i-1}$ is the velocity difference between the following car i and the leading car $i-1$.

FVDM behaves better than OVM and GFM in spite of its simplicity, as it takes more factors into account in car-following rules. However, there are still a few weaknesses in describing some pressing traffic conditions of FVDM.

4 Our Method

4.1 Overview

As illustrated in Figure 1, in our approach, given a time step, the following steps are executed to simulate vehicular flows.

Step 1: Before the simulation, we need to specify initial and boundary conditions, including initialization of position, velocity and so on.

Step 2: Use our introduced AA-FVDM method to compute acceleration for each vehicle except the leading one, and then compute the new velocity for the next time step.

Step 3: If there are vehicles that meet lane changing rules, we start those lane changes.

Step 4: Advance cars to next time step, using the computed information, update network state; jump to Step 2, and another cycle begins.

4.2 Accident-Avoidance FVDM

Our AA-FVDM is inspired by the FVDM [8] and crowd dynamics [29, 30], hence we start from a force perspective. To cope with the **close-car-braking circumstance**, we assume there is an elliptic range embracing each vehicle. Each car and its corresponding ellipse have the same center point on the horizontal plane. The semi-major axis r_i has a relation with the length of the corresponding car l_i, which is: $r_i = \gamma l_i$ (also mentioned in Section 3). If the distance $d_{i,i-1} = x_{i-1} - x_i$ between two nearest cars i and $i-1$ is smaller than the sum $r_{i,i-1} = r_i + r_i - 1$ of their semimajor axes, there will exist two kinds of interaction forces we called "psychological force" $f_2(i, i-1)$ and "body force" $f_3(i, i-1)$. $f_2(i, i-1)$ describes that a car will have a psychological tendency to keep away from another car if the distance between them is smaller than the safe interval. $f_3(i, i-1)$ is to counteract body compression of two neighboring ellipses in a lane. As a consequence, we add these two force terms into Eq. (2).

$$\begin{aligned}\frac{dv_i}{dt} &= \kappa[V(s_i) - v_i] - \lambda \Delta v_i \\ &\quad + f_2(i, i-1) + f_3(i, i-1)\end{aligned} \tag{3}$$

Both $f_2(i, i-1)$ and $f_3(i, i-1)$ should increase with decreasing distance $d_{i,i-1}$, but disappear if the distance $d_{i,i-1} \geq r_{i,i-1}$. This strategy is consistent with real-world traffic: the following vehicle will decelerate strongly to avoid accidents if the distance between it and the leader is small; the smaller the distance is, the larger the deceleration becomes.

Here,

$$\begin{aligned}f_2(i, i-1) &= -C\Theta(r_{i,i-1} - d_{i,i-1}) \\ &\quad \times e^{(r_{i,i-1} - d_{i,i-1})/D}\end{aligned} \tag{4}$$

$$\begin{aligned}f_3(i, i-1) &= -k\Theta(r_{i,i-1} - d_{i,i-1}) \\ &\quad \times H(r_{i,i-1} - d_{i,i-1})\end{aligned} \tag{5}$$

and $\Theta(x)$ is the Heaviside Function:

$$\Theta(x) = \begin{cases} 1 & x > 0 \\ 0 & else \end{cases} \tag{6}$$

together with,

$$H(x) = x \tag{7}$$

C, D, and k are certain positive constants, and in traffic simulation we set $C \in (0, 1]$, $k \in (0, 1]$, $D = \max(r_{i,i-1} - d_{i,i-1})$.

Based on our observation and the description of Helbing et al. [12], deceleration capabilities of vehicles are greater than acceleration capabilities, thus our approach is reasonable.

From Eq. (3), we can tell that our AA-FVDM degenerates to FVDM if there are no "psychological force" and "body force", and reduces to GFM regardless of negative effect of velocity difference and no added force terms are in effect. It also degrades to OVM if $\lambda = 0$, $f_2(i, i-1) = 0$, $f_3(i, i-1) = 0$.

4.3 Handling Lane Changes

4.3.1 Decision-Making on Lane Changes

Inspired by empirical observations, we propose a simple method in light of visual information, which is more or less similar to lots of related rules or models on decisions of whether performing a lane change.

Generally speaking, drivers try to make lane changes due to various motivations, for example, overtaking slow traffic, going to off-ramps, avoiding other cars, slowing down, making turns, road narrowing and for a variety of other reasons. In this study, we simply select overtaking, taking off-ramps as the main incentives. Besides, when changing to other lanes, the safety criteria (i.e. no collisions) should be guaranteed. We first introduce some variables before formulating the incentive criteria and safety criteria.

As illustrated in the following diagram (see Figure 2), v_r^h is the velocity of the leading car on the right-hand lane, v_l^h is the velocity of the ahead vehicle on the left-hand lane, v and pos are the speed and position of the car which considers making a lane change, v^h is the speed of the car ahead of the current car. Preference factor δ represents the preference of taking off-ramps when meeting an exit. $v_{\max}$ is the maximum speed on certain lane.

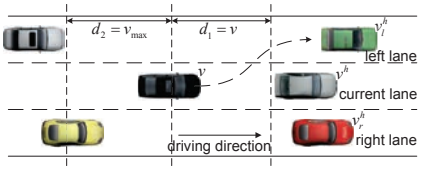

Figure 2: An illustration for making decisions of lane changes.

Incentive criteria: $v_r^h \geq \eta v^h$, $v_l^h \geq \eta v^h$, $v_r^h \geq \mu v$, $v_l^h \geq \mu v$ (overtaking incentive); $\delta \geq 0.8$ (exit ramps stimulation).

Safety criteria: the boundaries $[pos - v_{\max}, pos + v]$ ensure a safe distance on the target lane (i.e. the right lane or the left lane) with

taking the current position pos of the vehicle into account.

Note that if there is a long enough distance without any vehicles on the target lanes, it may be reasonable of the present car to perform a lane change. Under this situation, we set $v_r^h = v_{\max}$ or $v_l^h = v_{\max}$.

We assign each vehicle a probability P when these criteria are met. In other words, a car has a probability of $1 - P$ to stay in the current lane. In our implementation, $P \geq q$ ($q \in [0.7, 1.0]$) is stochastically prescribed for some cars which decide to perform lane changes.

4.3.2 Execution of Lane Changing Course

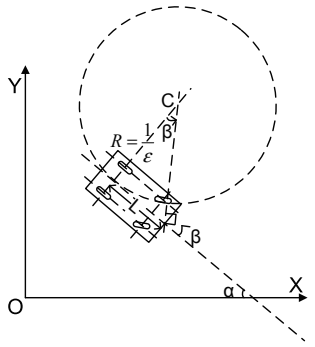

Figure 3: The dynamics of a lane-changing car. α is the direction relative to the X axis, β is the steering angle, ε and R are the curvature and the radius of the traveled path.

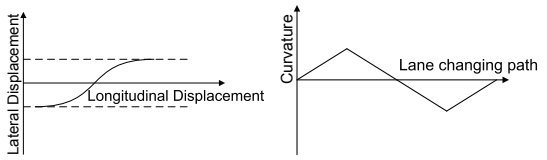

(a) (b)

Figure 4: (a) A lane-changing curve, and (b) its corresponding curvature whose derivative is constant.

After making a decision on changing lanes, the next step is to execute the lane changing course. Previous studies show that the lane changing maneuver was either modeled as an instantaneous event [1, 16–19], or an action with uniform duration [20], however, we aim to generate lifelike traffic animation, and a lane change needs several seconds according to real-life experience. An effective way is to approximate lane changing trajectory by a series of short lines. In this section, we present the process of lane changes at great length. The above scheme is an illustration describing the dynamics of a car which performs a lane change (see Figure 3).

First of all, it is necessary to make some derivations using discretization method within the time step period Δt.

$$\frac{\Delta d}{\Delta t} = v, \frac{\Delta v}{\Delta t} = a, \frac{\Delta \beta}{\Delta t} = \omega \tag{8}$$

where Δt is the time step length, Δd denotes the length of a small path segment during the lane changing procedure, Δv indicates the velocity difference, $\Delta \beta$ is the steering angle difference. d , v, and β are the traversed path length, the velocity, and steering angle of a car, respectively.

On the basis of the real-world traffic, or lane changing reasons, the velocity v, acceleration a, and the steering speed ω are all limited: $v \in (0, v_{\max}], a \in [0, a_{\max}], \omega \in [-\omega_{\max}, \omega_{\max}]$. The positive velocity assures that the current vehicle should only move forward. The corresponding acceleration is non-negative such that the car can make a lane change smoothly and steadily. If a vehicle decelerates during lane changes, the risks will increase a lot, thus probably leading to traffic accidents.

Regarding the length of the path segment Δd, we use it to compute the homologous curvature, several trigonometric functions, the new steering angle $\alpha(d + \Delta d)$, and the new coordinate values $x(d + \Delta d)$, $y(d + \Delta d)$.

$$\begin{aligned} \frac{\Delta \alpha}{\Delta d} &= \varepsilon = \frac{\tan \beta}{L} \\ \frac{\Delta x}{\Delta d} &= \sin \alpha, \frac{\Delta y}{\Delta d} = \cos \alpha \end{aligned} \tag{9}$$

Here, the computation of the curvature ε complies with its inherent definition, β is the steering angle with $|\beta| \leq \beta_{\max}$, and L is the distance between the rear axle and the front line of a vehicle (see Figure 3). Δx and Δy are the length variations with respect to the segment length along the X axis and Y axis, respectively. α is the lane changing direction relative to the X axis. x, y are coordinate values along the X, Y axes.

Note that a lane-changing curve is symmetric in its midpoint, due to the reversibility of the changing course. It is also notable that the curvature is zero at three points: the start point, the midpoint and the end point. Clearly, there are two curves between the start point and the end point: one with the maximum curvature which

is positive, and the other with the maximum curvature which is negative.

5 Results

All the results are collected on an Intel Core(TM) i7-3770 3.40 GHZ CPU with a high-end independent graphics card. The road network is extracted from the real world, including flyovers, tunnels, and suspension bridges.

5.1 Scenarios

We simulate traffic congestion and the scenario described in the **close-car-braking circumstance** (the corresponding numerical simulation is in Section 5.2.1), lane changing behavior, and traffic at on/off ramps. Please see the complementary videos.

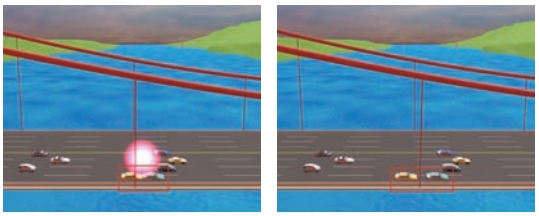

(a) Using FVDM. (b) Using our AA-FVDM.

Figure 5: Simulating scenarios for close-car-braking circumstance with FVDM, and our method under the same initial conditions, respectively. (a) is a screenshot using FVDM, and it indicates that a collision takes place. (b) is a snapshot by adopting our method. The result shows that our technique is capable of avoiding accidents.

(a) (b)

Figure 6: (a) A car at an interchange between two neighboring lanes. (b) A car entering a ramp.

5.1.1 Traffic Jams

From a practical perspective, jams usually occur when the leading vehicles decelerate for certain reasons. We simulate traffic congestion based on this fact (see complementary videos). Stop and go phenomenon also takes place along with traffic congestion.

5.1.2 Scenario for close-car-braking circumstance

As described above, FVDM cannot handle **close-car-braking circumstance**, however, our method is able to cope with this problem. We animate the same traffic flow with FVDM, and our technique, respectively. The visual results are presented below (see Figure 5).

5.1.3 Lane Changes

We merge lane changing behavior into our system, and Figure 6(a) shows the visual effects of lane changing behavior.

5.1.4 Traffic at on/off Ramps

In reality, ramp traffic is very common for choosing different driving directions. The flyover in our framework contains 8 on-ramps and 8 off-ramps. See Figure 6(b).

5.2 Performance

5.2.1 Comparison with FVDM

The situation is described as: the velocity of the leader and the follower are 20.0 m/s and 20.0 m/s at the beginning, and the initial netto interval (netto spacing) between them is 10 m; the leading car decelerates at -6 m/s^2 until it completely stops, and keep stopping for several seconds before speeding up to 21 m/s. We conduct 2 experiments under the same initial condition, employing FVDM and our method, respectively.

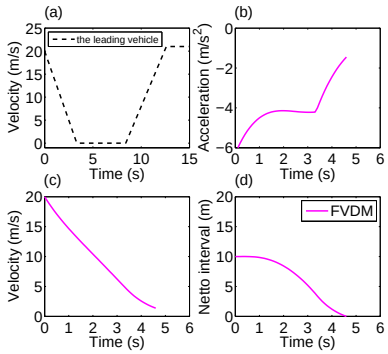

Figure 7: Simulations for FVDM in close-car-braking circumstance. (a) velocity of the leading vehicle, (b) deceleration of the following car, (c) speed of the following car, (d) the netto interval between the leader and the follower.

In such a situation, we can observe that FVDM is not capable of avoiding collisions or accidents, since it generates negative netto distance between the leading vehicle and the following vehicle, while the velocity of the follower is still

positive. The leader and the follower get into an accident at 4.6 s in the FVDM (see Figure 7).

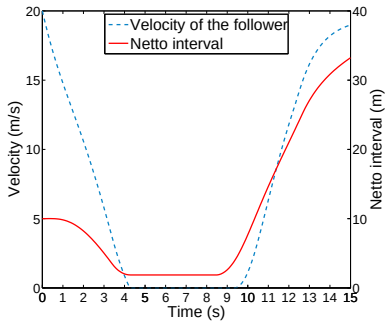

Figure 8: Simulations for AA-FVDM. With our method, the velocity of the follower can timely decelerate to zero to avoid collisions with the leader. The following car will accelerate if the leading vehicle moves again.

We also test our method under the same situation as presented above. The simulation results prove that the AA-FVDM is able to cope with such a problem without producing accidents (see Figure 8). We can see from Figure 8 that the minimal netto distance is roughly 2 m over the whole process. The follower with a small interval can timely decelerate to zero and avoid collisions when the leader brakes steeply for an accident.

5.2.2 Performance Tests

First, we test the update frequency of our method with FPS (Frames Per Second) and memory usage. Then we investigate how the percent of lane changing vehicles varies along with traffic density. Finally, we choose two typical parameters and perform some parameter tests, involving the probability variable q (Section 4.3.1) and the variable $r_{i,i-1}$ (Section 4.2). Each test has been run for a constant period with 80 times.

Without taking lane changing behavior into account (see Figure 9(a)), our method may update more than 185,000 vehicles in real time. The usage of memory increases linearly with the number of vehicles. An analogous linear growth can also be observed from Figure 9(b), however, with considering lane changes the maximum number of vehicles that can be updated at interactive rates is around 85,000, which is much less than that in Figure 9(a).

From real-world experience, we know that dense traffic will bring little opportunity for vehicles to perform lane changes. Our simulation results live up to this experience, which can be validated by Figure 10.

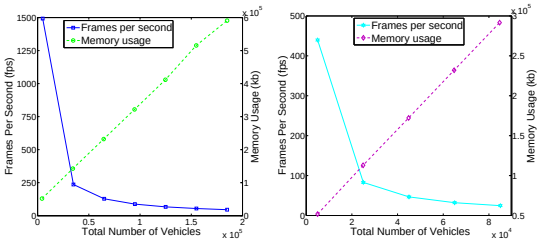

(a) (b)

Figure 9: (a) Frames per second and approximate memory usage for updating various numbers of vehicles without lane changing behavior. the update frequency is about 45 fps when there are 185,000 vehicles. (b) Frames per second and memory usage for differing numbers of vehicles with lane changing behavior. The update is roughly 25 fps when the number of vehicles is 85,000.

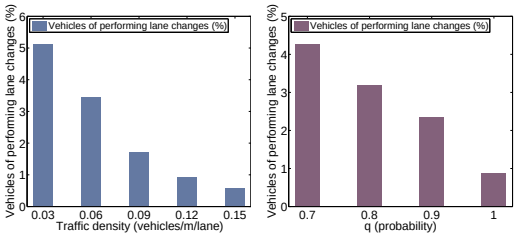

(a) (b)

Figure 10: (a) The percent of vehicles that perform lane changes along with traffic density. Vehicles performing lane changes occupy a greater percent when traffic becomes sparse.(b) The impact of probability (q) on percent of vehicles that make lane changes. A larger probability leads to a smaller lane changing percent of total vehicles.

The first parameter we test is the probability variable q (Section 4.3.1). We set the boundaries of q is $[0.7, 1.0]$ in this study, and we test $q = 0.7$, $q = 0.8$, $q = 0.9$, and $q = 1.0$ respectively. It is not hard to see that if $q = 0.7$, only vehicles assigned $P \geq 0.7$ can perform lane changing (these vehicles must meet the safety and incentive criteria). If $q = 1.0$, it means that vehicles whose probability must be $P = 1.0$

(a) $r_{i,i-1} = 15.0$ (b) $r_{i,i-1} = 20.0$ (c) $r_{i,i-1} = 25.0$ (d) $r_{i,i-1} = 30.0$

Figure 11: Parameter tests with different $r_{i,i-1}$, a longer $r_{i,i-1}$ results in a larger gap between the leading vehicle and the following vehicle.

may make lane changes. Therefore, a smaller q results in a larger percent of vehicles that perform lane changing behavior (see Figure 10). The second parameter that we choose is the variable $r_{i,i-1}$. The difference of $r_{i,i-1}$ leads to different results. From our method we can realize that a larger $r_{i,i-1}$ implies earlier repulsive forces between two nearest cars in the same lane. We test this idea in the same scenario, and the result (see Figure 11) reveals that a larger $r_{i,i-1}$ leads to a greater gap between the leader and the follower.

5.3 Verification with Real Traffic Data

In order to validate our method, we compute the standard deviations between simulation results and real-world traffic data (NGSIM) for different traffic models (MITSIM [31], IDM [32], GFM [12], FVDM [8] and our AA-FVDM), and make a comparison with the outcomes. We utilize an effective method called trust region algorithm (TRA) [33] since it provides a numerical solution to the problem of minimizing a function, generally nonlinear, over a space of parameters of the function.

To evaluate the results of different traffic models, we bring in the standard deviation, which is also named root mean square error (RMSE). A smaller RMSE indicates a better agreement with real traffic data. RMSE is computed as follows:

$$RMSE = \sqrt{\frac{\sum_{i=1}^{n}(E(\sigma_i) - \sigma_i)^2}{n-1}} \qquad (10)$$

where n denotes the sample size, in this study, we choose the vehicles' velocity as σ_i, $E(\sigma_i)$ is the computed value using traffic simulation models. We know that $v(t+\Delta t^{'}) = v(t)+a\Delta t^{'}$, in US101 datasets, the time step is 0.1 s, which only induces a small variation in velocity, therefore we choose 1 s as the time step size ($\Delta t^{'} = 1\ s$). Table 1 shows the RMSE of differing traffic models, Table 2 exhibits the resulting optimal parameters for our method.

In Figure 12, we can observe that all models except MITSIM compare well with real traffic data. MITSIM has a remarkable overshooting, which indicates too large accelerations. Our method has a similar trend as FVDM, because ours is on top of it. It is interesting that our method outperforms FVDM, even though there is a little difference, as shown in Table 1. Table 2 demonstrates that the parameters from the velocity function have analogous values to that in Helbing's work [12], which further validates our method.

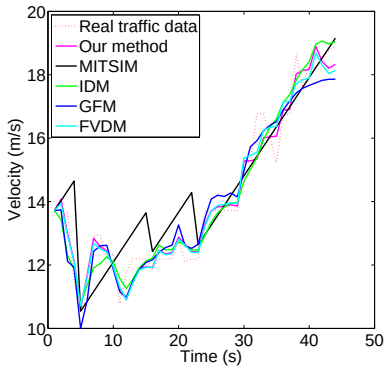

Figure 12: Comparison of real-world traffic data and simulated velocity using different traffic models.

Table 1: Minimal values of RMSE between real traffic data and simulation results that were reached for various traffic models by trust region algorithm.

Model	Ours	FVDM	IDM
RMSE	0.479	0.504	0.590
Model	GFM	MITSIM	
RMSE	0.604	1.007	

Table 2: The optimal parameter values for our method—AA-FVDM.

Parameters	$\kappa(s^{-1})$	$V_1(m/s)$	$V_2(m/s)$
Values	0.486	8.31	9.87
Parameters	$C_1(m^{-1})$	C_2	$\lambda(s^{-1})$
Values	0.155	1.212	0.421
Parameters	$r_{i,i-1}(m)$	$C(m/s^2)$	$k(s^{-2})$
Values	27.797	0.544	0.1

6 Conclusion and Future Work

We have set up a rural road web with diverse road structures including flyovers, suspension bridges, curving tunnels and other straight or curve roads. Currently, our system allows for differing vehicle types, diverse speed limits on various road segments, and supports lane changing behavior.

On the basis of FVDM, we have proposed a novel method inspired by force concept [29, 30], and is able to address some emergency (**close-car-braking circumstance**): the distance between two nearest vehicles is quite small, and the leader brakes sharply because of accidents ahead or others. However, the cost is that the new method may lead to overshooting deceleration when an emergency occurs. It is inevitable because when there is an emergency ahead, only strong deceleration can the current car cut its speed quickly and avoid accidents. We also represent simple rules, the kinetics and constraints on lane changing behavior. While believable and realistic lane changing behavior can be simulated with our technique, one restriction is that we did not consider vehicles' types when performing a lane change, for example, a truck should need a longer lane change than a small car.

Then we conduct differing experiments to test the AA-FVDM. Due to the agent-based property of our method, the update duration is much longer than continuum-based models. However, our method can simulate anisotropic drivers, individualistic behavior with complex dynamics. Furthermore, the performance is fairly good, and it is able to simulate tens of thousands vehicles with our method at interactive rates. Above all, we validate our method using real-world traffic data, and compare with other traffic methods. The matching results show that our method remarkably outperforms others (FVDM, IDM, GFM, MITSIM).

However, there are still some restrictions in our current framework. In line with the reality that passing rules are differing in diverse areas such as USA, China and Germany, lane changes can be classified into two classes: asymmetric and symmetric. We plan to simulate both types in different scenarios. Another limit is that our current system does not support path planning for an individual vehicle, and vehicles choose random directions at intersections. Even though there was some work for simulating both pedestrians and traffic flows [34], it focused on pedestrians and just presented very simple traffic flows. So we may simulate crowds and vehicles in great detail. These points are not currently considered in our prototype system, and they can be investigated in the next step.

Acknowledgements

This research is supported by Natural Science Foundation of China (Grant 60970125 and 61202207), China Postdoctoral Science Foundation (Grant 2012M520067).

References

[1] Sumo - simulation of urban mobility, 2012. http://sumo.sourceforge.net/.

[2] M.J. Lighthill and G.B. Whitham. On kinematic waves. ii. a theory of traffic flow on long crowded roads. *Proceedings of the Royal Society of London. Series A. Mathematical and Physical Sciences*, 229(1178):317–345, 1955.

[3] P. I. Richards. Shock-waves on the highway. *Operations Research*, 4(1):42–51, 1956.

[4] H.J. Payne. Models of freeway traffic and control. *Mathematical models of public systems*, 1971.

[5] A. Aw and M. Rascle. Resurrection of "second order" models of traffic flow. *Siam Journal on Applied Mathematics*, 60(3):916–938, 2000.

[6] H. M. Zhang. A non-equilibrium traffic model devoid of gas-like behavior. *Transportation Research Part B-Methodological*, 36(3):275–290, 2002.

[7] J. Sewall, D. Wilkie, P. Merrell, and M. C. Lin. Continuum traffic simulation. *Computer Graphics Forum*, 29(2):439–448, 2010.

[8] R. Jiang, Q. S. Wu, and Z. J. Zhu. Full velocity difference model for a car-following theory. *Physical Review E*, 64(1), 2001.

[9] D.L. Gerlough. *Simulation of freeway traffic on a general-purpose discrete variable computer*. PhD thesis, University of California, Los Angeles, 1955.

[10] G. F. Newell. Nonlinear effects in the dynamics of car following. *Operations Research*, 9(2):209–229, 1961.

[11] M. Bando, K. Hasebe, A. Nakayama, A. Shibata, and Y. Sugiyama. Dynamical model of traffic congestion and numerical simulation. *Physical Review E*, 51(2):1035–42, 1995.

[12] D. Helbing and B. Tilch. Generalized force model of traffic dynamics. *Physical Review E*, 58(1):133–8, 1998.

[13] S. Algers, E. Bernauer, M. Boero, L. Breheret, CD Taranto, M. Dougherty, K. Fox, and JF Gabard. Smartest project: Review of micro-simulation models. *EU project No: RO-97-SC*, 1059(2), 1997.

[14] D. Helbing. Traffic and related self-driven many-particle systems. *Reviews of Modern Physics*, 73(4):1067–1141, 2001.

[15] K. Nagel and M. Schreckenberg. A cellular automation model for freeway traffic. *Journal De Physique I*, 2(12):2221–2229, 1992.

[16] P. G. Gipps. A model for the structure of lane-changing decisions. *Transportation Research, Part B (Methodological)*, 20B(5):403–14, 1986.

[17] K.I. Ahmed, M. Ben-Akiva, H.N. Koutsopoulos, and R.G. Mishalani. Models of freeway lane changing and gap acceptance behavior. In *Proceedings of the 13th international symposium on the theory of traffic flow and transportation*, pages 501–515. Pergamon New York, NY, 1996.

[18] Q. Yang and H. N. Koutsopoulos. A microscopic traffic simulator for evaluation of dynamic traffic management systems. *Transportation Research Part C-Emerging Technologies*, 4(3):113–129, 1996.

[19] A. Kesting, M. Treiber, and D. Helbing. General lane-changing model mobil for car-following models. *Transportation Research Record: Journal of the Transportation Research Board*, 1999(-1):86–94, 2007.

[20] P. Hidas. Modelling vehicle interactions in microscopic simulation of merging and weaving. *Transportation Research Part C-Emerging Technologies*, 13(1):37–62, 2005.

[21] S. Moridpour, M. Sarvi, and G. Rose. Lane changing models: A critical review. *Transportation Letters: The International Journal of Transportation Research*, 2(3):157–173, 2010.

[22] Jur van den Berg, Jason Sewall, Ming Lin, and Dinesh Manocha. *Virtualized Traffic: Reconstructing traffic flows from discrete spatio-temporal data*. IEEE Virtual Reality 2009, Proceedings. 2009.

[23] Jason Sewall, David Wilkie, and Ming C. Lin. Interactive hybrid simulation of large-scale traffic. *ACM Transactions on Graphics*, 30(6), 2011.

[24] I. Prigogine and F. C. Andrews. A boltzmann-like approach for traffic flow. *Operations Research*, 8(6):789–797, 1960.

[25] P. Nelson, DD Bui, and A. Sopasakis. A novel traffic stream model deriving from a bimodal kinetic equilibrium, 1997.

[26] V. Shvetsov and D. Helbing. Macroscopic dynamics of multilane traffic. *Physical Review E*, 59(6):6328–6339, 1999.

[27] K. Nagel, D. E. Wolf, P. Wagner, and P. Simon. Two-lane traffic rules for cellular automata: A systematic approach. *Physical Review E*, 58(2):1425–37, 1998.

[28] D. W. Huang. Lane-changing behavior on highways. *Physical Review E*, 66(2), 2002.

[29] D. Helbing and P. Molnar. Social force model for pedestrian dynamics. *Physical Review E*, 51(5):4282–6, 1995.

[30] D. Helbing, I. Farkas, and T. Vicsek. Simulating dynamical features of escape panic. *Nature*, 407(6803):487–490, 2000.

[31] Mitsim. mit intelligent transportation systems, 2012. http://mit.edu/its/mitsimlab.html.

[32] M. Treiber, A. Hennecke, and D. Helbing. Congested traffic states in empirical observations and microscopic simulations. *Physical Review E*, 62(2):1805–1824, 2000.

[33] T. F. Coleman and Li Yuying. An interior trust region approach for nonlinear minimization subject to bounds. *SIAM Journal on Optimization*, 6(2):418–45, 1996.

[34] Adrien Treuille, Seth Cooper, and Zoran Popovic. Continuum crowds. *ACM Transactions on Graphics*, 25(3):1160–1168, 2006.